Pergamon

Int. J. Heat Mass Transfer. Vol. 39, No. 9, pp. 1797–1803, 1996

0017-9310/96 $15.00+0.00

0017-9310(95)00291-X

Cold heat-release characteristics of phase-change emulsion by air–emulsion direct-contact heat exchange method

HIDEO INABA

Department of Mechanical Engineering, Faculty of Engineering, Okayama University, Tsushimanaka 3-1-1, Okayama 700, Japan

and

SHIN-ICHI MORITA

Sunwave-Industry Inc., Hayase 1-11-25, Saitama 338, Japan

(*Received* 15 *March* 1995 *and in final form* 24 *July* 1995)

Abstract—This paper deals with cold heat-release characteristics of the oil (tetradecane, $C_{14}H_{30}$, latent heat 229 kJ/kg, melting point 278.9 K)/water emulsion as a latent heat-storage material having a low melting point. An air–emulsion direct-contact heat exchange method was selected for the cold heat-release from the emulsion layer including solidified tetradecane. The temperature effectiveness, the sensible heat release time and the latent heat release time were measured as experimental parameters. The useful nondimensional correlation equations for those parameters were derived in terms of nondimensional emulsion layer depth, expressed the emulsion layer dimension, Reynolds number for air flow, Stefan number and heat capacity ratio.

1. INTRODUCTION

The fine latent heat storage material–water mixture has fluidity even if the dispersed fine latent heat-storage material having a higher freezing point than water is frozen, because the mixture includes the unfreezing of water as the continuum phase. The authors have already reported the physical properties (density, specific heat, latent heat, thermal conductivity and viscosity) [1–3] and the latent cold heat storage characteristics [2] of oil (tetradecane, $C_{14}H_{30}$, latent heat $L = 229$ kJ/kg, melting point $T_m = 278.9$ K)/water emulsion as the fine latent heat storage material–water mixture. The latent cold heat storage material can supply the cold heat at constant temperature in the vicinity of its melting point during the latent heat release. The hot–cold emulsion direct contact heat exchanger is selected as the latent cold heat release method from dispersed–solidified fine tetradecane droplets in the emulsion.

Kato *et al.* [4] investigated the gas hold-up, bubble size, interfacial area, longitude dispersion coefficient of liquid and volumetric coefficient of mass transfer in a bubble column. The heat transfer coefficient between the dispersion air bubble in fine solid particle–water mixture and a vertical heating surface was evaluated by Mersmann *et al.* [5]. The experimental study of the air–hot water direct contact heat exchanger was performed on air bubble size and heat transfer coefficient between air bubbles and hot water by authors [6].

The latent heat release system by the hot air–latent heat emulsion direct contact heat exchanger is evaluated in the present paper. The mass fraction of tetradecane as the dispersed latent cold heat storage material, the height of the emulsion layer in the test heat exchanger, the initial temperature of emulsion, the inlet hot air temperature and the velocity of inlet hot air are selected as the experimental parameters.

2. CHARACTERISTICS OF PHASE-CHANGE EMULSION

Table 1 indicates the mass fraction of the test emulsion. The emulsion consists of tetradecane C_t (mass%) as the fine latent cold heat storage material, the water C_w (mass%) as the continuum phase and the surfactant C_s (mass%). The emulsion shows stable dispersion mixing by using the surfactant which consists of anionic surfactant and nonionic surfactant. The anionic surfactant and the nonionic surfactant are in the mass ratio of one to ten. The diameter of the dispersion tetradecane varies from $d = 0.1$ to 9.0 μm, the arithmetic mean diameter is $d_m = 3.4$ μm, and the standard deviation is $\pm 20.4\%$ [1]. The experimental data evaluation is carried out using the physical properties (density, specific heat, latent heat and thermal conductivity of the test emulsion) measured by

NOMENCLATURE

a_a	thermal diffusivity of air [$m^2 s^{-1}$]
a_e	thermal diffusivity of emulsion [$m^2 s^{-1}$]
A_n	area of nozzle [m^2]
A_{ves}	circular bottom area of test section [m^2]
Cp_a	specific heat of air [kJ $(kg \cdot K)^{-1}$]
Cp_e	specific heat of emulsion [kJ $(kg \cdot K)^{-1}$]
C_t	mass fraction of tetradecane [mass %]
C_s	mass fraction of surfactant [mass %]
C_w	mass fraction of water [mass %]
d	diameter of dispersed tetradecane [μm]
d_n	diameter of nozzle [mm, m]
d_{ves}	diameter of test section [mm, m]
Fo_l	Fourier number of latent heat-release time
Fo_s	Fourier number of sensible heat-release time
h^*	heat capacity ratio
L	latent heat of tetradecane [kJ kg^{-1}]
L_e	latent heat of emulsion [kJ kg^{-1}]
m_e	mass of emulsion [kg]
$\dot{m}_a$	mass flow rate of air [kg s^{-1}]
n	number of nozzle
P_{cr}	phase change rate defined by equation (3) [%]
Q_{tot}	total release heat [kJ]
Q_l	released latent heat [kJ]
Q_s	released sensible heat [kJ]
Q_{los}	heat loss, based on the temperature difference between emulsion layer and atmospheric temperature [kJ]
Re	Reynolds number defined by equation (7)
Ste	Stefan number defined by equation (12)
t	time [s, min]
t_l	latent heat-release time [s, min]
t_s	sensible heat-release time [s, min]
T_{ain}	inlet air temperature [K]
T_{aout}	outlet air temperature [K]
T_e	emulsion temperature [K]
T_{ei}	initial emulsion temperature [K]
T_m	melting point of tetradecane (278.9 K) [K]
T_w	temperature of water [K]
u_n	air velocity from a nozzle $(= V/(n \times A_n))$ [m s^{-1}]
$\dot{V}$	volume flow rate of air [$m^3 s^{-1}$]
z	emulsion layer depth [m, mm]
z^*	nondimensional emulsion layer depth.

Greek symbols

ν_a	kinematic viscosity of air [$m^2 s^{-1}$]
ϕ_a	temperature effectiveness
ψ_a	relative humidity of air [%].

Subscripts

a	air
ain	inlet air
aout	outlet air
e	emulsion
i	initial
l	latent heat
los	heat loss
m	melting point, mean
max	maximum
s	sensible heat
ves	test section of the vessel.

Table 1. Mass fraction of emulsion

Tetradecane C_t [mass %]	Water C_w [mass %]	Surfactant C_s [mass %]
40.0	49.3	10.7
35.0	56.0	9.0
25.0	66.7	8.3
15.0	78.5	6.5

Inaba *et al.* [1]. Table 2 shows the representatively thermophysical properties of the emulsion at $T_e = 275.1$ K.

3. EXPERIMENTAL APPARATUS AND PROCEDURES

Figure 1 shows the experimental apparatus for the latent cold heat-release experiment from the emulsion layer which includes the frozen fine tetradecane droplets. The dispersed tetradecane droplets in the emulsion are frozen by the cold latent heat storage apparatus, which consists mainly of a coiled double tube heat exchanger [2]. The experimental apparatus consists of the cylindrical vessel (test section, 89 mm in inside diameter, 500 mm in height, 3.0 mm in thickness), the rectangular vessel (cross-section of 180 mm in width × 180 mm in depth, 500 mm in height and 20 or 10 mm in thickness) and the nozzles which are set in the bottom of the test section. The space between the cylindrical vessel and the rectangular vessel is kept at a vacuum of 7.99 kPa in pressure by a vacuum pump, and the rectangular vessel is thermally insulated by the uretan foam insulating material (50 mm in thickness). The air flow rate and temperature are controlled by the flow controller and an electric heater, respectively. The measuring accuracy of the

Table 2. Thermophysical properties of test emulsion at $T_e = 275.1$ K

Emulsion C_t [mass %]	Density [kg m^{-3}]	Specific heat [kJ (kg·K)$^{-1}$]	Thermal conductivity [W (m·K)$^{-1}$]
40.0	908	3.13	0.46
35.0	919	3.27	0.47
25.0	942	3.52	0.50
15.0	965	3.78	0.51

air flow rate is within $\pm 3\%$ of the maximum flow rate ($\dot{V}_{max} = 9.13 \times 10^{-4}$ m^3 s^{-1}). The temperatures of the emulsion layer are measured by T-type thermocouples of 0.1 mm in diameter. The inlet and outlet air temperatures of the test section are measured by thermopiles which are constructed by five T-type thermocouples of 0.1 mm in diameter. The thermocouples are calibrated by a standard thermometer within ± 0.05 K. The thermopile for the outlet air temperature of the test section can be traversed in the height direction from the emulsion layer and it is set the center of cylindrical test section, since the outlet air temperature distribution in the radical direction over the test emulsion layer is small within ± 0.3 K. The inlet and outlet air humidity are measured by the electric hygrometer (measuring range of relative humidity $\psi_a = 0 \sim 90\%$, accuracy $\pm 3\%$). The air nozzles (diameter $d_n = 2.0$ mm, number of nozzles $n = 49$) are arranged at intervals of 10 mm in the radial direction and 30° in the circumference direction. The air nozzle diameter $d_n = 2.0$ mm is determined by the experimental results in which the foaming phenomenon by the surfactant does not occur during air injection in the emulsion layer. Tetrafluoroethylene resin filter (residue particle diameter 2.0 μm, 0.5 mm in thickness) is mounted at the bottom of the air nozzles in order to protect the emulsion leakage. The inlet hot air temperature T_{ain} and air velocity $u_n (= \dot{V}/(n \times (\pi/4) d_n^2))$ are controlled within ± 0.1 K and $\pm 1.08 \times 10^{-2}$ m s^{-1} of each experimental condition, respectively. The cold heat transferred by the mass transfer of humidity is less than 4% of the total released cold heat. The relative humidity of inlet air is controlled $\psi_a = 5 \sim 20\%$ in the present experiment. The air hold-up in the emulsion layer is fairly large, so that the maximum depth ($z = 241$ mm) of the emulsion layer is restricted to about half the depth of the test rectangular vessel. The experimental parameters range as follows:

- air velocity from nozzle $u_n = 1.48 \sim 5.93$ m s^{-1};
- inlet hot air temperature $T_{ain} = 303.1 \sim 318.1$ K;
- tetradecane mass fraction of emulsion $C_t = 15.0 \sim 40.0$ mass%;
- height of emulsion layer $z = 32 \sim 241$ mm;
- initial emulsion temperature $T_{ei} = 273.6 \sim 277.9$ K.

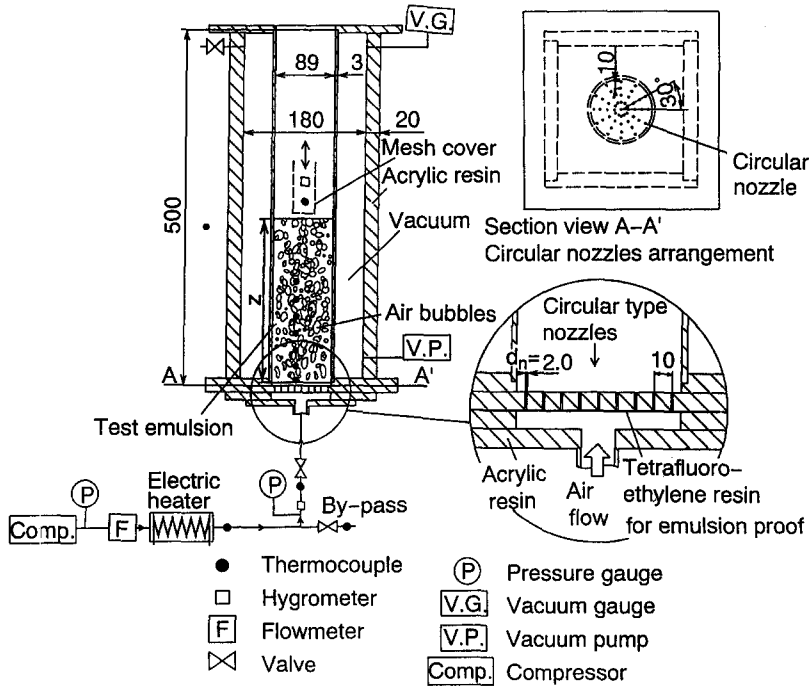

Fig. 1. Experimental apparatus for cold heat-release.

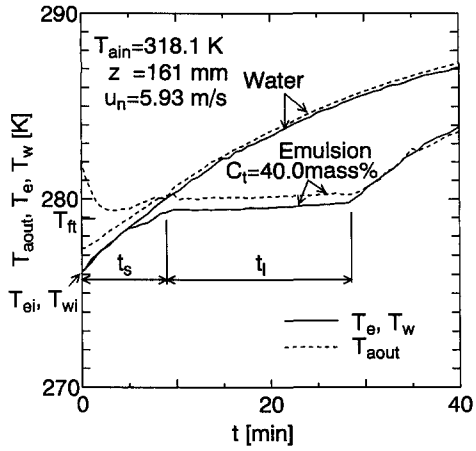

Fig. 2. Variation of water temperature T_w, emulsion (C_t = 40.0 mass%) temperature T_e and outlet air temperature T_{aout} with time t.

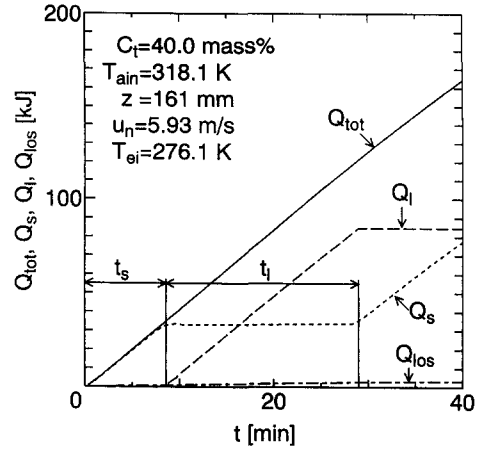

Fig. 3. Variation of total release-heat Q_{tot}, sensible release-heat Q_s, latent release-heat Q_l and heat loss Q_{los} with time t.

4. EXPERIMENTAL RESULTS AND DISCUSSIONS

Figure 2 shows the time history of water temperature T_w, emulsion temperature T_e (C_t = 40.0 mass%) and outlet air temperature T_{aout}. The various time histories of temperatures as shown in Fig. 2 indicate the experimental results of only water and the emulsion, respectively. The maximum temperature difference of the emulsion in the emulsion layer is within 1 K, because air bubbles mix the emulsion. The outlet air temperature T_{aout} of the only cold water in the test section increases monotonously with time t. However, T_{aout} value of the emulsion shows a decreasing tendency at the beginning, subsequently it shows constant one due to the latent cold heat release, and finally it increases. The decrease of T_{aout} at the beginning is caused by the low air bubble velocity in the emulsion layer due to high viscosity of the emulsion. The low bubble velocity takes a long time to arrive at the surface of emulsion layer, so that T_{aout} decreases at the beginning of experiment. T_{aout} during latent cold heat release process shows slightly higher than the emulsion temperature T_e. This temperature difference is brought by the heat resistance between the surfactant micelle and dispersed phase-change tetradecane.

The sensible heat release time t_s at the beginning and the latent heat release time t_l are indicated in Fig. 2. The t_s and the t_l are estimated by the heat balance of test emulsion layer, which is calculated by the following equation

$$Q_{tot} = \int Cp_a \times \dot{m}_a \times (T_{ain} - T_{aout})\,dt = Q_l + Q_s + Q_{los} \tag{1}$$

in which Q_{tot} is total release heat of emulsion, Cp_a is specific heat of air, $\dot{m}_a$ is mass flow rate of air, T_{ain} is inlet air temperature, T_{aout} is outlet air temperature, Q_l is latent release heat, Q_s is sensible release heat and Q_{los} is heat loss. That is, the times t_s and t_l are defined as the times estimated when the integrated sensible and latent cold heats absorbed by air bubbles are coincident with the beforehand calculated sensible and latent cold heats released from the emulsion.

The sensible release heat Q_s is calculated by

$$Q_s = Cp_e \times m_e \times (T_e - T_{ei}) \tag{2}$$

using each value of specific heat of emulsion Cp_e, mass of emulsion m_e, emulsion temperature T_e and initial emulsion temperature T_{ei}.

The heat loss Q_{los} based on the temperature difference between the emulsion and atmospheric temperature is measured at the preparatory experiment by using a cold water as the test fluid. The quantity of heat loss Q_{los} is less than 3% of the total storage heat of the emulsion. The variation of Q_{tot}, Q_s, Q_l and Q_{los} with time t is shown in Fig. 3.

Figure 4 presents the time history of the phase-change rate of P_{cr} of the emulsion. The phase-change rate P_{cr} is defined by the released latent heat Q_l and latent heat of the emulsion L_e as follows:

$$P_{cr} = \frac{Q_l}{m_e \times L_e} \times 100 = \frac{Q_l}{m_e \times (C_t/100) \times L} \times 100, \tag{3}$$

where L is latent heat of tetradecane (L = 229 kJ/kg). The P_{cr} increases linearly with time t in the latent heat

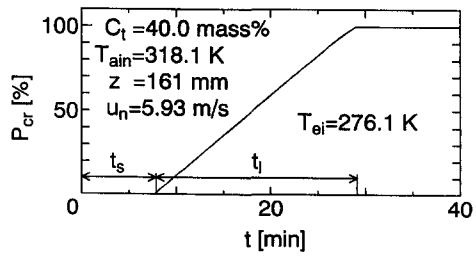

Fig. 4. Time history of phase change rate P_{cr} or solidified tetradecane in the emulsion.

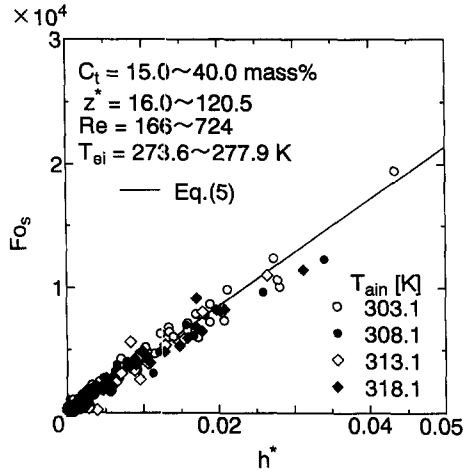

Fig. 5. Relationship between Fourier number Fo_s of sensible heat-release time and heat capacity ratio h^*.

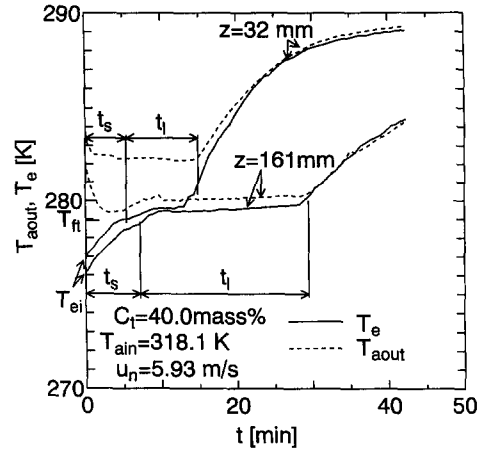

Fig. 6. Time history of emulsion ($C_t = 40.0$ mass%) temperature T_e and outlet air temperature T_{aout} on emulsion layer depth $z = 32$ mm and 161 mm.

release process, since the high heat exchange effectiveness between the hot air and the emulsion can be obtained by the direct contact heat exchange.

Figure 5 illustrates the relationship between Fourier number Fo_s ($= a_e \times t_s/d_n^2$) expressing sensible heat release time t_s and the nondimensional heat capacity ratio h^*. The sensible heat release time t_s is expressed by Fourier number Fo_s as nondimensional parameter of time which is commonly used. The heat capacity ratio h^* is defined as follows:

$$h^* = \frac{Cp_e \times m_e \times (T_m - T_{ei}) \times a_e}{Cp_a \times \dot{m}_a \times (T_{ain} - T_m) \times A_{ves}}, \tag{4}$$

where A_{ves} ($= (d_{ves}/2)^2\pi$) is the bottom surface area of test section vessel.

The Fo_s number increases linearly with an increase in the heat capacity ratio h^*. The Fo_s number is derived in terms of h^*, as follows:

$$Fo_s = 4.29 \times 10^5 \times h^*. \tag{5}$$

The calculated value by equation (5) is equal within $\pm 9.9\%$ of the experimental data. The application range of equation (5) is $C_t = 15.0 \sim 40.0$ mass%, $z^* = 16.0 \sim 120.5$, $Re = 166 \sim 724$, $T_{ain} = 303.1 \sim 318.1$ K and $T_{ei} = 273.6 \sim 277.9$ K, $A_{ves} = 6.22 \times 10^{-3}$ m^2. The nondimensional emulsion layer depth z^* and Reynolds number Re are defined as follows:

$$z^* = \frac{z}{d_n}, \tag{6}$$

$$Re = \frac{u_n \times d_n}{\nu_a} \tag{7}$$

in which z is emulsion layer depth in the test section, d_n ($= 2.0$ mm) is diameter of nozzle and ν_a is kinematic viscosity of air.

Figure 6 shows the variation of T_{aout} and T_e ($z = 32$ mm, 161 mm) with time t. The latent heat release time t_l of $z = 32$ mm is shorter than that of $z = 161$ mm since the total latent heat decreases with a decrease in the emulsion layer depth z. Temperature difference between T_{aout} and T_e in the latent heat release process increases with a decrease in emulsion layer depth z due to a decrease of staying time of the air bubbles in the emulsion layer. The outlet air temperature in the latent heat release process is an important factor for this type of latent release system estimation. The relationship between temperature effectiveness ϕ_a and nondimensional emulsion layer depth z^* is shown in Fig. 7.

The temperature effectiveness ϕ_a is defined as follows:

$$\phi_a = \frac{T_{ain} - T_{aout}}{T_{ain} - T_m}, \tag{8}$$

where T_{aout} is the time average temperature during the latent cold heat release process. The temperature

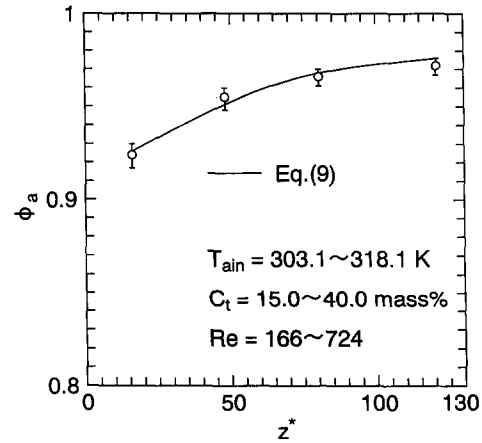

Fig. 7. Variation of temperature effectiveness ϕ_a with nondimensional emulsion layer depth z^*.

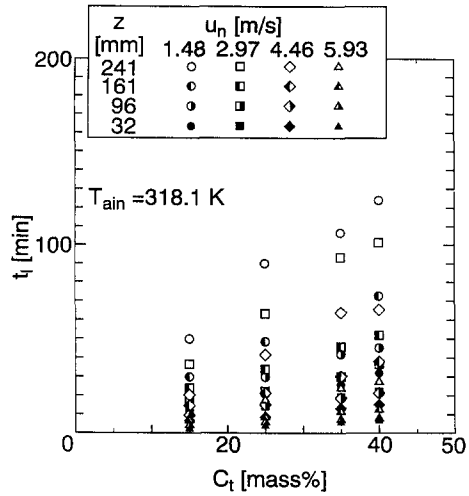

Fig. 8. Relationship between latent heat-release time t_l and mass fraction of tetradecane C_t.

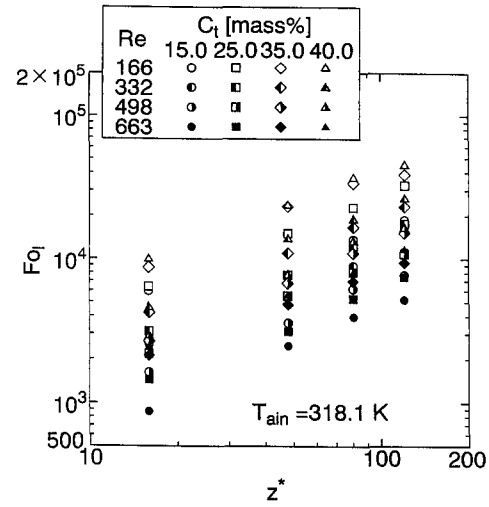

Fig. 9. Variation of Fourier number Fo_l of latent heat-release time with nondimensional emulsion layer depth z^*.

effectiveness becomes $\phi_a = 0.92$ or more, and it increases with increasing nondimensional emulsion layer depth z^*. This tendency of ϕ_a with z^* is explained by the fact that the amount of exchanging heat between the hot air bubbles and the emulsion increases with an increase in z^*, due to the increase of air staying time of ascending air bubbles, as shown in Fig. 7. The relationship between ϕ_a and z^* is derived with a function of z^* within the standard deviation of $\pm 7.2\%$ as follows:

$$\phi_a = -4.26\times10^{-6}z^{*2} + 1.06\times10^{-3}z^* + 0.911. \tag{9}$$

Figure 8 indicates the relationship between the latent heat-release time t_l of the emulsion and the mass fraction of tetradecane C_t at $T_{ain} = 318.1$ K. From this figure, it is revealed that the t_l increases with an increase in the emulsion layer depth z and mass fraction of tetradecane C_t, and with decreasing in air velocity u_n from a nozzle.

Figure 9 shows the variation of Fourier number Fo_l $(= t_l \times a_e/D_n^2)$ with nondimensional emulsion layer depth z^*. The latent heat release time t_l is nondimensionalized by Fourier number Fo_l. The Fo_l number increases with an increase in z^*, since the amount of latent heat of the emulsion increases with an increase in the emulsion layer depth z. The relationship between Fo_l number and z^* in equation (10) can be obtained by the least mean squares method as follows:

$$Fo_l \propto z^{*0.822}. \tag{10}$$

The variation of Fo_l number with Reynolds number Re is demonstrated in Fig. 10. The Fo_l number decreases with an increase in the Re number. This tendency is explained by the fact that the increase of Re number brings an increase in the amount of air bubbles. The decreasing rate of Fo_l number against Re number is obtained by the least squares method as follows:

$$Fo_l \propto Re^{-1.02}. \tag{11}$$

The relationship between Fo_l number and Stefan number Ste is shown in Fig. 11. The Ste number is defined as follows:

$$Ste = \frac{Cp_e \times (T_{ain} - T_m)}{(C_t/100)\times L}. \tag{12}$$

The Ste number is the nondimensional parameter which expresses the ratio of sensible heat of the emulsion to the latent heat. The relationship between Fo_l number and Ste number is expressed by

$$Fo_l \propto Ste^{-0.747}. \tag{13}$$

All the data concerning Fo_l number are plotted with

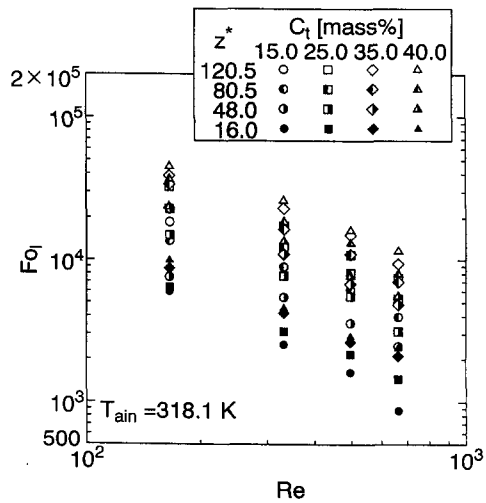

Fig. 10. Relationship between Fo_l number and Reynolds number Re.

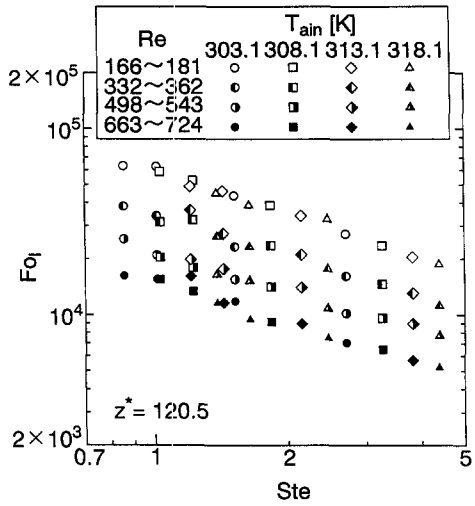

Fig. 11. Variation of Fo_l number with Stefan number Ste.

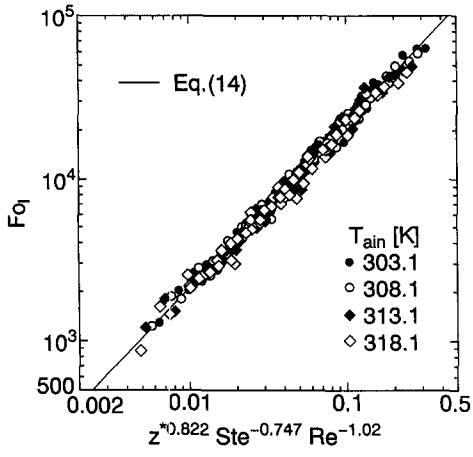

Fig. 12. Relationship between Fo_l number and $z^{*0.822}Ste^{-0.747}Re^{-1.02}$.

the function of $z^{*0.822}\ Ste^{-0.747}\ Re^{-1.02}$ and with the relationship in equations (10), (11) and (13), as shown in Fig. 12. The solid line in Fig. 12 indicates the experimental correlation equation (14) which is derived within the standard deviation of $\pm 9.5\%$ by the least squares method as follows:

$$Fo_l = 2.28 \times 10^5 \times z^{*0.822} Ste^{-0.747} Re^{-1.02}. \quad (14)$$

The applicable range of equation (14) refers to $C_t = 15.0 \sim 40.0$ mass%, $T_{ain} = 303.1 \sim 318.1$ K, $Ste = 0.86 \sim 4.43$, $z^* = 16.0 \sim 120.5$ and $Re = 166 \sim 724$. The total heat release time $(t_s + t_l)$ can be calculated from the sum of Fo numbers in equations (5) and (14).

5. CONCLUDING REMARKS

The cold heat-release experiment of the emulsion, including the phase-change material (tetradecane) as the dispersion medium, has been carried out by the hot air–emulsion direct contact heat exchange method. Important factors for the estimation of phase-change emulsion heat-release system are investigated experimentally. Consequently, some conclusions are obtained as follows:

(1) The temperature of the outlet air after the heat exchange approaches the tetradecane melting point with increasing emulsion layer depth. As a result, it is understood that very high temperature effectiveness can be obtained in the present direct-contact heat exchange system. The temperature effectiveness can be derived in terms of nondimensional emulsion layer depth.

(2) The useful correlation equations of Fourier number expressing the nondimensional heat-release time for sensible and latent heat process are proposed in terms of heat capacity ratio, nondimensional emulsion layer depth, Reynolds number and Stefan number.

Acknowledgements—The authors would like to acknowledge the help received from Mr M. Fujisaki, undergraduate student, Department of Mechanical Engineering, Okayama University.

REFERENCES

1. H. Inaba, S. Morita and S. Nozu, Fundamental study of cold heat-storage system of O/W-type emulsion having cold latent-heat-dispersion material (1st report, estimation of thermophysical properties), *JSME* **59-565** 2882–2889 (1993) (in Japanese).
2. H. Inaba and S. Morita, Fundamental study of cold heat-storage system of O/W-type emulsion having cold latent-heat-dispersion material (2nd report, flow and cold heat-storage characteristics of emulsion in a coiled double-tube heat exchanger), *JSME* **60-572,** 1422–1429 (1994) (in Japanese).
3. H. Inaba, S. Morita and S. Nozu, Viscosity evaluation of O/W emulsion as a low temperature heat storage material, *JSTP* **7-4,** 239–244 (1993) (in Japanese).
4. Y. Kato, A. Ishimaru, H. Kadone and S. Morooka, Characteristics of bubble column with a simultaneous gas-liquid injection nozzle, *Kagaku-kogaku* **6-6,** 614–621 (1980) (in Japanese).
5. A. Mersmann, H. Noth, D. Ringer and R. Wunder, Maximum heat transfer in equipment with dispersed two-phase systems, *Int. Chem. Engng* **22-1,** 16–29 (1982).
6. H. Inaba, *et al.*, Heat mass transfer characteristics by a direct contact between air bubbles and hot water, 31*st JSME Cyugoku-Sikoku Area Conference*, Vol. 935-1, pp. 178–180 (1993) (in Japanese).